Photoisomerisation and ligand-controlled reversible aggregation of azobenzene-functionalised gold nanoparticles

Electronic Supplementary Information (ESI)

Anja Köhntopp, Alexandra Dabrowski, Michal Malicki and Friedrich Temps

S1. Syntheses

The functionalised gold nanoparticles (AuNPs) were synthesised in a two-step process starting from oleylamine-stabilised AuNPs followed by ligand exchange with the selected azothiol and respective alkylthiol. The oleylamine-stabilised AuNPs were obtained following a variant of the protocol described in Ref. S1. The azoligands 4-(11-mercaptoundecanoxy)-azobenzene (AB-OC11SH), 4-(7-mercaptoheptanoxy)-azobenzene (AB-OC7SH) and 4-(3-mercaptopropanoxy)-azobenzene (AB-OC3SH) were synthesised via a slightly modified three-step procedure adopted from Klajn et al.[S2] The synthesis of AB-OC11SH is described as example below, the other azothiols were obtained accordingly.

The integrity and purity of all intermediate and final products was carefully checked by NMR spectroscopy. Contrary to occasional other reports, we did not observe reduction of the azobenzene groups in the presence of the thiol groups during our syntheses, but oxidation of the thiols to disulfides may occur. However, as disulfides also bind to Au surfaces (with dissociation of the disulfide bond), the presence of disulfides poses no serious problem for our syntheses. According to our NMR measurements, the oxidation is slow at room temperature and played no significant role within the time frame of our synthesis.

S1.1 4-(Undec-10-enyloxy)-azobenzene

4-Hydroxyazobenzene (2.11 g, 10.7 mmol) and potassium *tert*-butoxide (1.25 g, 11.1 mmol) were placed in a three-neck round bottom flask equipped with a reflux condenser. The setup was purged with argon for 10 min, followed by the addition of 25 mL of dry DMF. The mixture was stirred at room temperature until the solid reactants had dissolved. Next, 11-bromo-1-undecene (2.50 mL, 11.1 mmol) was added and the mixture was heated to reflux for 25 min, during which the colour of the solution changed to bright red and a colourless precipitate formed. The reaction was monitored by TLC (silica gel, hexane/ethyl acetate (20:1)). After cooling down to room temperature the reaction mixture was poured into 100 mL of deionized water and the aqueous solution was extracted with *n*-hexane (4 × 50 mL). The combined hexane fractions were washed with water (4 × 50 mL) and dried over magnesium sulfate. The solvent was evaporated under reduced pressure to yield an orange solid, which was recrystallized from ethanol. The product was obtained as an orange crystalline solid (2.42 g, 65 %).

^{1}H-NMR (200 MHz, $CDCl_3$): δ = 7.95–7.83 (m, 4H, Ar-H), 7.54–7.40 (m, 3H, Ar-H), 7.04–6.96 (m, 2H, Ar-H), 5.82 (ddt, ^3J = 16.9 Hz, ^3J = 10.1 Hz, ^3J = 6.6 Hz, 1H, C*H*=CH_2), 5.05–4.89 (m, 2H, =CH_2), 4.04 (t, ^3J = 6.5 Hz, 2H, -O-CH_2), 2.05 (m, 2H), 1.82 (m, 2H), 1.55–1.27 (m, 12H) ppm.

S1.2 4-(11-Thioacetoxyundecanoxy)-azobenzene

4-(Undec-10-enyloxy)-azobenzene (1.01 g, 2.87 mmol) and azobisisobutyronitrile (141 mg, 0.86 mmol) were placed in a three-neck round bottom flask equipped with a reflux condenser. The flask was purged with argon for 25 min followed by the addition of 20 mL of dry toluene and thioacetic acid (810 µL, 11.44 mmol) while stirring. The reaction mixture was refluxed for 2 h, after which the reaction mixture was cooled down to room temperature. The mixture was then poured into a separatory funnel containing 100 mL of saturated sodium hydrogen carbonate solution and 50 mL of toluene. The organic phase was separated and washed with 50 mL saturated sodium hydrogen carbonate solution, followed by washing with deionized water (5 × 50 mL). The solution was dried over magnesium sulfate and the solvent was evaporated under reduced pressure. The obtained orange solid was recrystallized from methanol. The product was obtained as an orange crystalline solid (974 mg, 80 %).

^{1}H-NMR (200 MHz, $CDCl_3$): δ = 7.95–7.83 (m, 4H, Ar-H), 7.54–7.39 (m, 3H, Ar-H), 7.04–6.96 (m, 2H, Ar-H), 4.04 (t, ^3J = 6.5 Hz, 2H, -O-CH_2), 2.92–2.79 (m, 2H), 2.32 (s, 3H, CH_3), 1.90–1.74 (m, 2H), 1.65–1.25 (m, 16H) ppm.

S1.3 4-(11-Mercaptoundecanoxy)-azobenzene (AB-OC11SH)

4-(11-Thioacetoxyundecanoxy)-azobenzene (950 mg, 2.30 mmol) was placed in a three-neck round bottom flask, which was purged with argon for 20 min. Then 20 mL of degassed methanol and 5 mL of a 1 M solution of HCl in methanol were added. The reaction mixture was heated to reflux for 6 h after which the reaction mixture was cooled to room temperature. The precipitate which had formed during the reaction was filtered off, washed with a small amount of cold methanol and dried in vacuo. The procedure yielded a yellow powdery solid (805 mg, 94 %).

^{1}H-NMR (500 MHz, $CDCl_3$): δ = 7.93–7.86 (m, 4H, Ar-H), 7.52–7.41 (m, 3H, Ar-H), 7.02–6.98 (m, 2H, Ar-H), 4.04 (t, ^3J = 6.6 Hz, 2H, -O-CH_2), 2.52 (dd, ^3J = 14.7 Hz, ^3J = 7.4 Hz, 2H, -CH_2-SH), 1.86–1.78 (m, 2H, -O-CH_2-CH_2), 1.61 (dt, ^3J = 14.8 Hz, ^3J = 7.3 Hz, 2H, -CH_2 -CH_2-SH), 1.52–1.44 (m, 2H), 1.42–1.25 (m, 12H), 1.33 (t, ^3J = 7.5 Hz, 1H, -SH) ppm.

S1.4 Oleylamine-stabilised AuNPs

Hydrogen tetrachloroaurate trihydrate (200 mg, 0.51 mmol) was dissolved in a mixture of 2.00 mL of toluene and 2.00 mL of freshly distilled oleylamine. This solution was poured into a mixture of 15.0 mL of toluene and 4.00 mL of oleylamine in a 100 mL round bottom flask. 2.00 mL of methanol were added to the solution. Next, sodium borohydride (41.0 mg, 1.08 mmol) was added to the mixture at once while stirring. Immediately after addition of sodium borohydride the reaction mixture turned dark. It was stirred vigorously at room temperature for 2 – 2.5 h. Next the reaction mixture was poured into 35 mL of acetonitrile resulting in a dark precipitate. The precipitate was washed first with acetonitrile (3 × 20 mL), and then with methanol (3 × 20 mL). The particles were then redissolved and used without further characterization for the ligand exchange reaction. The above procedure usually yielded ≈ 100 mg of oleylamine-coated AuNPs.

S1.5 Ligand exchange

To exchange the oleylamine against thiol ligands a known amount of oleylamine-coated AuNPs was dissolved in toluene yielding a solution with concentration of approximately 2.5 mg/mL. The solution was then degassed with Ar for 20 min. Next, a two-fold excess of a mixture of the azothiol ligand and the alkylthiol coligand dissolved in degassed toluene was added at once. The required amounts of thiol for the ligand exchange were estimated before the reaction from the NP diameter determined by the TEM measurements and the resulting surface area assuming a value for the thiol surface footprint on the NPs of F_{thiol} = 22 Å^2/molecule.[S3] The azothiol mole fractions in the ligand exchange mixtures were between x_{AB} = 0.3 – 0.7 (mostly mixtures with x_{AB} = 0.5 were used). The total amount of toluene was chosen such that the final AuNP concentration was ≈ 2 mg/mL. The reaction mixture was kept under Ar atmosphere and was stirred at room temperature in the dark for ≈ 20 h. The NPs were then precipitated by addition of methanol and washed five times with a mixture of methanol and toluene (4:1). For the shorter chain lengths (AB-OC7SH and AB-OC3SH), the reaction mixtures were concentrated under vacuum before precipitation to reduce the necessary amount of methanol. The cleaned NPs were then dissolved in toluene.

S1.6 Materials

Oleylamine (Aldrich) was distilled under reduced pressure and stored under Ar atmosphere before use. $HAuCl_4 \cdot 3\,H_2O$ (Aldrich), $NaBH_4$ (Fluka), pentanethiol (Aldrich) and decanethiol (Aldrich) were used as purchased. All solvents were distilled under reduced pressure before use.

S2. NP characterisation

S2.1 Methods

For TEM imaging, performed at the Institute of Materials Science of Christian-Albrechts-University Kiel, toluene solutions of the AuNPs were drop-casted onto holey carbon grids and images were recorded at several acceleration voltages between 75 and 390 kV.

NMR spectra of the free azothiols and the AB-functionalised AuNPs were recorded on a Bruker DRX 500 or a Bruker AV 600 FT spectrometer in deuterated solvents.

UV/Vis absorption spectra were recorded on a Shimadzu UV-2401PC desktop spectrometer in fused silica cuvettes with 1 mm optical path length. Each spectrum was referenced to that of the pure solvent.

S2.2 NMR spectra at different AB surface coverages

The measured NMR spectra of AB-OC11S-/C10S-functionalised AuNPs prepared with different azothiol mole fractions are shown in Fig. S1. The spectrum of the free azoligand in solution serves as reference. The strong broadening of the ^{1}H resonances on the AuNPs is immediately evident. The observed high-field shift of the aromatic proton signals with increasing AB surface concentration supports an irregular, statistical distribution of the azothiolate and alkylthiolate ligands in the monolayer.

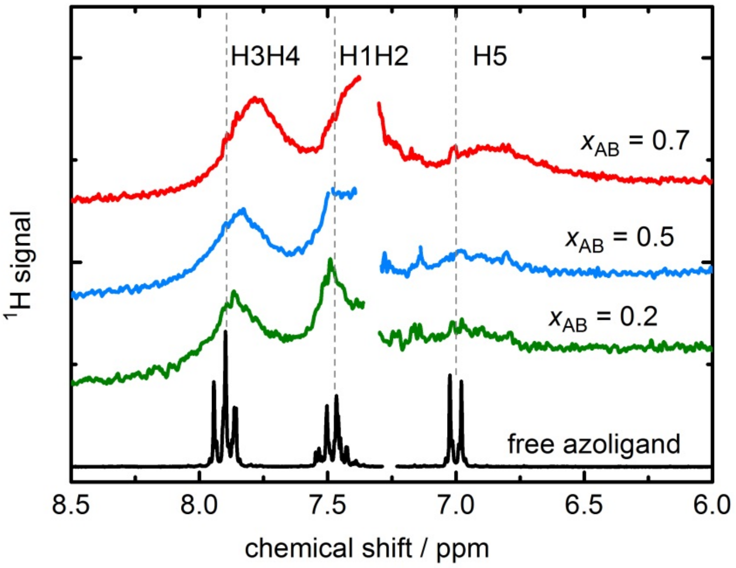

Fig. S1. ^{1}H NMR spectra in CD_2Cl_2 of AB-OC11S-/C10S-functionalised AuNPs prepared with different azothiol mole fractions. The spectrum at the bottom shows the positions of the aromatic ^{1}H signals of free AB-OC11SH in solution (see Section S1.3 for precise chemical shift values and assignments). The gap in the spectra around 7.3 ppm is due to a trace of chloroform which was cut out.

S2.3 Estimation of the AB surface coverage of the NPs from the UV/Vis spectra

The concentration (in mol/L) of the NPs in solution was estimated from the measured absorbance at the center of the LSPR band taking the empirical value for the decadic molar absorption coefficient of the AuNPs of

$$\varepsilon_{\mathrm{NP}} = 4.2 \times 10^4 \times d^{3.4}\ \mathrm{L\,mol^{-1}\,cm^{-1}}$$

with the particle diameter *d* in nm.[S4–S7] The number of Au atoms per NP is simply given by

$$N = \frac{\pi}{6}\frac{\rho_{Au} N_A}{M_{Au}} d^3$$

where ρ_{Au} = 19.3 g/mol is the macroscopic density of gold, M_{Au} = 197 g/mol is the molar weight, N_{A} is Avogadro's number, and *d* the nanoparticle diameter. For the AuNPs with $d \sim 4$ nm ($N \sim 2000$) studied in the present work, the molar absorption coefficient thus becomes

$$\varepsilon_{\mathrm{NP}} = 4.58 \times 10^6\ \mathrm{L\,mol^{-1}\,cm^{-1}}$$

which corresponds to a value of $\varepsilon_{1\mathrm{Au}} = 2.29 \times 10^3\ \mathrm{L\,mol^{-1}\,cm^{-1}}$ per Au atom. Considering the very small size of the investigated well-defined AuNPs of interest here, light scattering can be neglected compared to absorption under the applied experimental conditions as long as there is no aggregation, but scattering may contribute to the extinction (sum of absorption plus scattering) in the case of photo-induced aggregation below.

The concentration of attached azothiolate ligands on the AuNPs was derived after subtraction of the absorbance by the AuNPs themselves from the measured absorbance in the ππ* band at λ = 345 nm using the independently determined value for the molar absorption coefficient of the free AB ligands in solution of $\varepsilon_{\mathrm{AB}}$ = 26 200 L mol^{-1} cm^{-1}. Note that we assume here that the AB absorption coefficient on the AuNPs is not substantially altered by surface enhancement effects (as confirmed below, cf. Section S2.4).

A set of UV/Vis spectra illustrating the procedure is given in Fig. S2. Taking the experimental absorbance values for the example shown and the given absorption coefficients, we find an azothiolate surface coverage of ~125 molecules/AuNP. With the AuNP surface area of ~5000 Å^2/NP and the assumption of similar sticking probabilities for AB-OC7S- and C10S-ligands (x_{AB} = 0.5), this result corresponds to a surface footprint of ~20 Å^2/molecule in satisfactory agreement with accepted values.[S3]

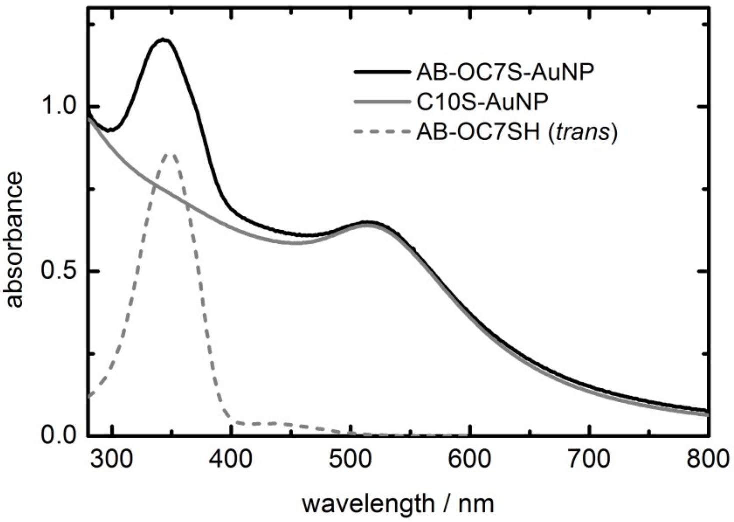

Fig. S2. UV/Vis absorption spectra of AB-OC7S-/C10S-functionalised AuNPs (solid black line) prepared using an equimolar solution (i.e. x_{AB} = 0.5) of AB-OC7SH and C10SH for the ligand exchange and C10S-functionalised AuNPs (solid grey line) in toluene at 1 mm optical pathlength. For comparison, the dashed grey line shows the absorption spectrum of free AB-OC11SH ($c = 3.2 \times 10^{-4}$ mol L^{-1}) in toluene. Light scattering can be neglected for the measured AuNPs here due to their small size.

S2.4 Estimation of the AB surface coverage on the NPs from NMR spectra

As surface enhancement effects may lead to an overestimation of the concentration of attached ligands from the UV/Vis absorption spectra, we used ^{1}H NMR spectroscopy as an independent alternative method to determine the AB concentration (Fig. S3). For these measurements, ethylene glycol (EG) was added to the sample as a standard of known concentration. Comparison of the integral of the EG signal at 3.66 ppm with the integral of the aromatic AB proton signals yielded the AB concentration in the sample. For identical concentrations of EG and AB ligand in the sample solution, the ratio of both integrals should be 9H/4H. As the measured integral corresponds to 16 protons, we find the concentration of AuNP-attached ABs to be 1.78 times the EG concentration of $c_{EG} = 0.89 \times 10^{-3}$ mol L^{-1}, which gives c_{AB}(NMR) = 1.58×10^{-3} mol L^{-1}.

From the UV/Vis absorption spectrum of the same sample solution, an AB concentration of c_{AB}(UV/Vis) = 1.38×10^{-3} mol/L was calculated. Within the estimated error limits of 25 % on both values, the AB concentrations obtained via ^{1}H NMR and via UV/Vis spectroscopy are thus seen to match well, indicating that – at least in the present case – there is no large change of the $\pi\pi^*$ band absorption strength of the AB ligands by surface enhancement effects on attachment of the ligands to the AuNPs.

Taking the AuNP concentration of $c_{NP} = 1.62 \times 10^{-5}$ mol L^{-1} in the same solution derived by UV/Vis spectroscopy (cf. Section 2.3), we calculate an azothiolate surface coverage of ~97

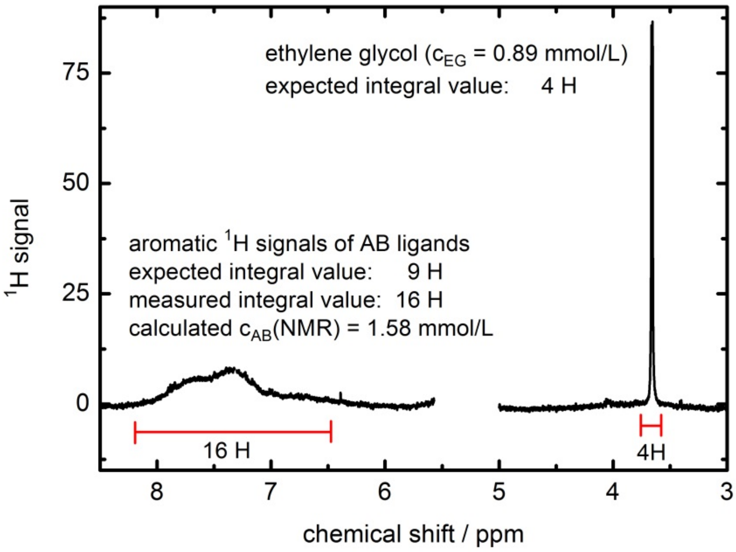

Fig. S3. ^{1}H NMR spectrum (baseline corrected) of AB-OC7S/C10S-AuNPs with ethylene glycol at c_{EG} = 0.89 mmol/L added as concentration standard. As the integral of the AB signal is 16 / 9 = 1.78 times larger than expected for equal concentrations of AB and ethylene glycol, the AB concentration is estimated to be c_{AB}(NMR) = 1.58 mmol/L.

molecules/AuNP from the NMR data compared to ~85 molecules/AuNP from the UV/Vis data. The latter value is a bit lower than the one for AB-OC11S-ligands determined in Section 2.3 above, reflecting unavoidable variations in the synthesis yields and a possible weak dependence on alkyl spacer chain lengths.

S3. Photoswitching

For the photoswitching experiments, the AB-functionalized AuNPs in solution in toluene were irradiated using two light emitting diodes with emission maxima at λ = 365 nm (NCSU033A, 400 mW) and λ = 455 nm (NS4C107E, 400 mW), respectively. All measurements were performed at room temperature.

S3.1 Photoswitching behaviour of non-aggregating AB-AuNPs

Photoswitching experiments were carried out with light at λ = 365 nm and λ = 455 nm to drive the AB-functionalised NPs from the *trans* to the *cis* and from the *cis* to the *trans* states, respectively. The measured behaviour of a typical sample of AB-OC7S-/C10S-functionalised AuNPs is illustrated in Fig. S4. The UV/Vis spectra after selected times of UV or Vis irradiation and in the respective photostationary states (PSS365 and PSS455) are displayed in panels A and B, while panels C and D show plots of the absorbance values at λ = 345 nm in the ππ* absorption band against irradiation time. As can be seen, the PSS365 (*trans-cis* isomerisation) is approached quite rapidly, similar to the case for the *trans-cis* photoisomerisation of the free azothiols in solution. The PSS455 (*cis-trans* isomerisation) takes longer to reach due to the much weaker absorption at the latter wavelength in the nπ*

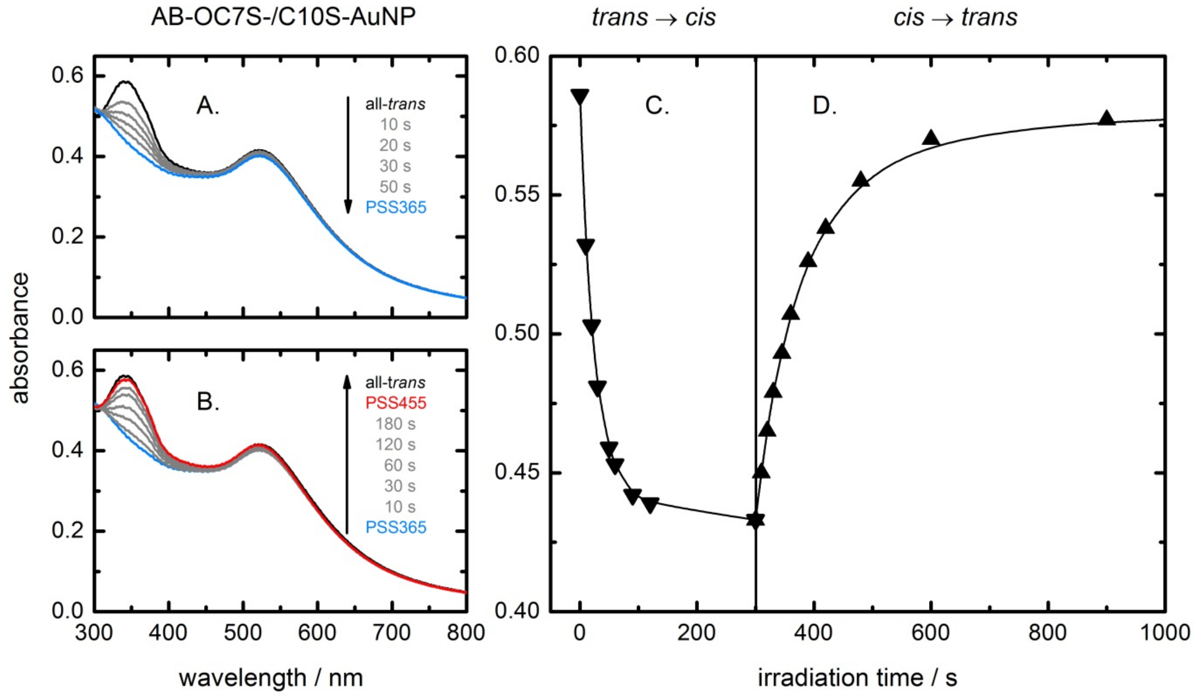

Fig. S4. Photoswitching behaviour of AB-OC7S-/C10S-functionalised AuNPs. A: UV/Vis spectra during irradiation at 365 nm (*trans-cis* isomerisation). B: UV/Vis spectra during irradiation at 455 nm (*cis-trans* isomerisation). C and D: Absorbance values at the maximum of the ππ* absorption band plotted against irradiation time.

band. The photo-induced isomerisation at 455 nm also appears to be slower because most of the incident light is absorbed by the AuNPs themselves rather than by the AB ligands. The observed halftimes for approach to the photostationary states are ~20 s (PSS365) and ~60 s (PSS455). To ensure that the photostationary states were really reached within experimental errors, and to rule out slower secondary photo-induced processes, however, the experiments were usually continued for longer times (up to 20 – 30 min) until the measured absorbances remained constant. Control measurements with 60 min irradiation times revealed no further change.

S3.2 Photoswitching behaviour of aggregating AB-AuNPs

As revealed by Fig. 2 in the main paper, AB-functionalised AuNPs with short alkylthiolate coligands exhibit photoreversible aggregation when the AB is switched to the *cis* state. In this case, the measured UV/Vis spectra show the overall extinction resulting from absorption and a possible contribution from light scattering. The behaviour of a typical aggregating sample is shown in Figs. S5 A and B for unstirred and in Figs. S5 C and D for stirred conditions. It is apparent that aggregation occurs and is fully photoreversible in both cases. However, the aggregation process seems to be slower in the stirred than in the unstirred case. At a given concentration, stirring should rather facilitate aggregation than prevent it. In the present case, however, the measurement under stirred condition has been performed

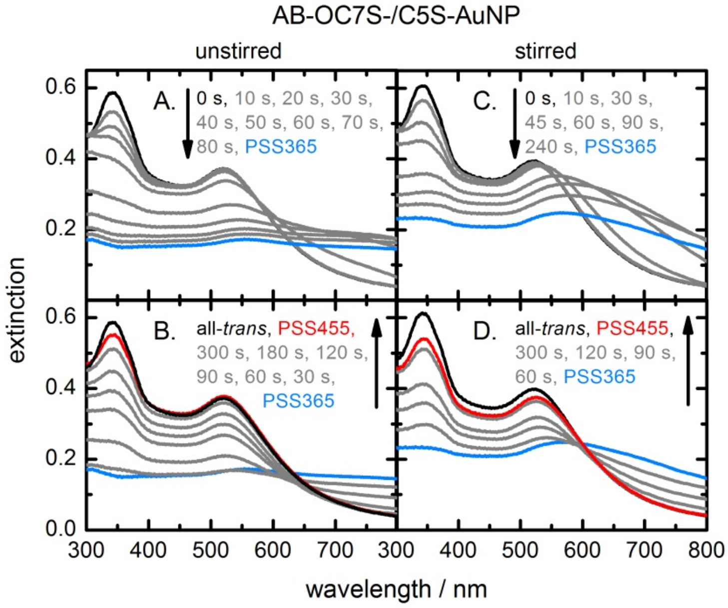

Fig. S5. Photoswitching behaviour of AB-OC7S-/C5S-functionalised AuNPs under unstirred conditions (A, B) and stirred conditions (C, D). A and C: extinction spectra during irradiation at 365 nm (*trans-cis* isomerisation); B and D: extinction spectra during irradiation at 455 nm (*cis-trans* isomerisation). The stirred measurements were performed at a ten-fold lower concentration in a 10 mm cuvette compared to the unstirred measurements performed in a 1 mm cuvette.

at ten-fold lower concentration in a cuvette with 10 mm pathlength than the measurement under unstirred conditions. Thus, the slower aggregation in the stirred case is fully expected on the grounds of the lower concentration.

S3.3 Increasing aggregation potential with higher AB surface coverage

Measured UV/Vis extinction spectra (absorption plus possible small contribution from scattering) of AB-OC7S/C5S-functionalised AuNPs with increasing number of attached azothiols (N_{AB}) from different syntheses are given in Fig. S6. An increasing strong broadening of the LSPR absorption feature indicating stronger aggregation with higher azothiol surface concentration from left to right is immediately recognisable.

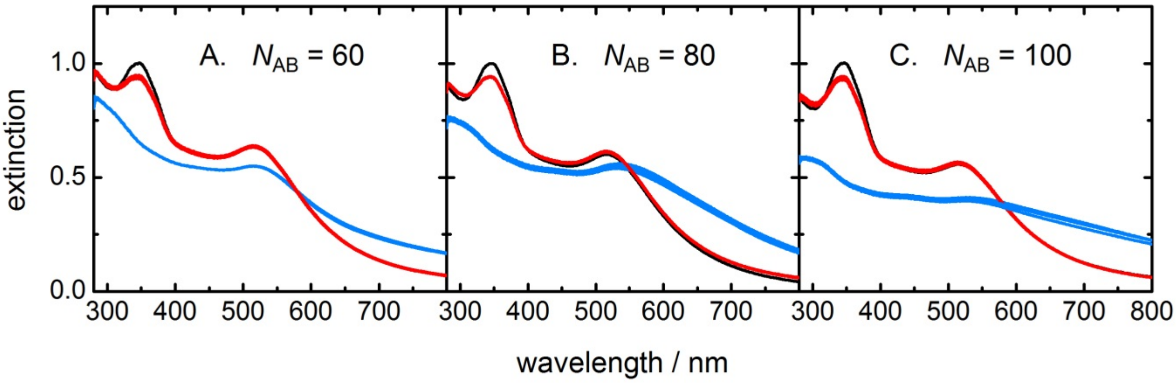

Fig. S6. UV/Vis extinction spectra of AB-OC7S/C5S-functionalised AuNPs with increasing number of attached azothiols (N_{AB}) from different syntheses. Spectra before irradiation (all-*trans*): black; in PSS365 (ABs mostly in *cis* form): blue; in PSS455 (ABs mostly back in *trans* form): red. Each panel shows the recorded spectra taken during 3 – 5 photoisomerisation cycles plotted on top of each other to point out that the samples can be switched back and forth between the two photostationary states reversibly and highly reproducibly.

S3.4 Estimation of the *trans*/*cis* compositions in the photostationary states

In order to determine the *trans*/*cis* compositions in the photostationary states PSS365 and PSS455, the measured UV/Vis spectra of the respective AB-AuNPs were modeled by the sum of the spectra of the alkylthiolate NPs and the spectra of *trans*-AB and *cis*-AB NPs according to

$$A_{\mathrm{AB-AuNP}} = A_{\mathrm{alkylS-AuNP}} + x_{trans} \times A_{trans} + (1 - x_{trans}) \times A_{cis}$$

using the molar fraction x_{trans} as adjustable fit parameter. The required spectrum of the free *cis*-AB thiol was derived from the spectrum in the PSS365 (mostly *cis*-AB) and the spectrum of the free *trans*-AB taking a value for the *trans*/*cis* ratio in the PSS365 derived by ^{1}H NMR spectroscopy.

The evaluation of the *trans*/*cis* ratios in the photostationary states is illustrated by Fig. S7. For the example shown, the results are

$$x_{\text{trans}} = 0.05 \pm 0.02,\ \ x_{\text{cis}} = 0.95 \pm 0.02 \text{ in PSS365}$$

and

$$x_{\text{trans}} = 0.80 \pm 0.05,\ \ x_{\text{cis}} = 0.20 \pm 0.05 \text{ in PSS455.}$$

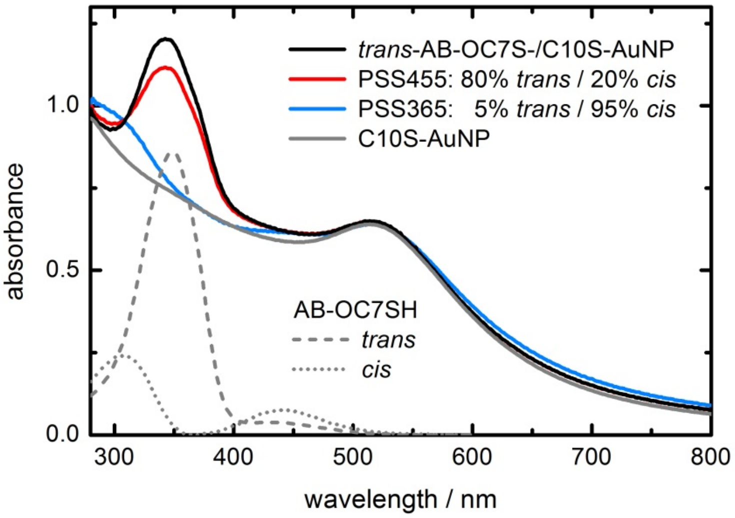

Fig. S7. UV/Vis spectra of AB-OC7S/C10S-functionalised AuNPs before irradiation (solid black line), in the PSS365 (solid blue line), in the PSS455 (solid red line) and UV/Vis spectra of decanethiolate-functionalised NPs (C10S-AuNPs, solid grey line). The dashed and dotted grey lines (bottom left) show the spectra of free *trans*-AB-OC7SH and *cis*-AB-OC7SH in solution, respectively.

S4. Thermal lifetimes for *cis*-AB ligands on AuNPs

The thermal lifetimes of the *cis*-azothiols in solution and the *cis*-azothiolate ligands on the AuNPs at room temperature are compiled in Table S1. As shown, the lifetimes of *cis*-ABs are not significantly altered on the AuNPs compared to AB in solution in case of the two longer ligand chains. For the shortest linker chain (AB-OC3SH) the *cis*-lifetime is reduced to half its value upon attachment to the AuNP.

Table S1. Thermal lifetimes of the investigated *cis*-AB ligands in solution and on the AuNP surface.

	$\tau_{\text{free AB}}$ / h	$\tau_{\text{AB-AuNP}}$ / h
AB-OC3SH	28	14
AB-OC7SH	19	17
AB-OC11SH	35	43

S5. References

S1. M. Malicki, J. M. Hales, M. Runi, S. R. Barlow, L. McClary, S. R. Marder and J. W. Perry, *Phys. Chem. Chem. Phys.* 2010, **12**, 6267.

S2. R. Klajn, P. J. Wesson, K. J. M. Bishop and B. A. Grzybowski, *Angew. Chem. Int. Ed.* 2009, **48**, 7035.

S3. F. Schreiber, *Prog. Surf. Sci.* 2000, **65**, 151.

S4. S. Link and M. A. El-Sayed, *J. Phys. Chem. B* 1999, **103**, 8410.

S5. P. K. Jain, K. S. Lee, I. H. El-Sayed and M. A. El-Sayed, *J. Phys. Chem. B* 2006, **110**, 7238.

S6. X. Liu, M. Atwater, J. Wang and Q. Huo, *Colloid. Surface. B* 2007, **58**, 3.

S7. G. A. Rance, D. H. Marsh and A. N. Khlobystov, *Chem. Phys. Lett.* 2008, **460**, 230.